

THE ENERGY SOURCES POWERING THE LATE-TIME BOLOMETRIC EVOLUTION OF SN 1987A

NICHOLAS B. SUNTZEFF,¹ M. M. PHILLIPS,¹ J. H. ELIAS,¹ D. L. DEPOY,² AND A. R. WALKER¹

Received 1991 September 16; accepted 1991 October 22

ABSTRACT

New optical and infrared data show that a third radioactive nuclide, ^{57}Co , is now powering the supernova nebula. The best fit to the late-time bolometric light curve is with $0.01 M_{\odot}$ ^{57}Co (~ 5 times the amount expected based on the solar ratio of $^{57}\text{Fe}/^{56}\text{Fe}$). However, if recent theoretical upper limits on the expected production of ^{57}Co and ^{44}Ti are correct, then either an additional energy input is needed or one of the fundamental assumptions used in the modeling of the data is in error. If a pulsar is present in the center of SN 1987A, it can be providing no more than $\sim 8 \times 10^{36}$ ergs s^{-1} on day 1500.

Subject headings: Magellanic Clouds — nucleosynthesis — stars: supernovae: general

1. INTRODUCTION

The bolometric evolution of SN 1987A through day 800 since outburst has been shown to be well fit by energy from radioactive nuclides produced in the supernova explosion deposited in a medium of slowly decreasing optical depth to gamma and X-rays. The energy input from $\sim 0.07 M_{\odot}$ of radioactive ^{56}Ni synthesized in the supernova explosion, which quickly decayed into radioactive ^{56}Co (Suntzeff & Bouchet 1990, hereafter SB90), is in excellent agreement with theoretical models (Woosley 1988; Shigeyama, Nomoto, & Hashimoto 1988; Woosley, Pinto, & Hartmann 1989, hereafter WPH89). By day 950, the bolometric decline began to slow (Walker & Suntzeff 1989), and by day 1350, an additional energy source was clearly present (Suntzeff et al. 1991, hereafter S91; Bouchet, Danziger, & Lucy 1991a).

We have previously reported our results (S91) on the bolometric evolution (often called the “uvoir” bolometric luminosity, since it is based on the “ultraviolet-optical-infrared” energy flux, which does not include the flux escaping in gamma and X-rays) of SN 1987A through day 1350, where we found that the bolometric evolution could be fit by a model with $0.071 M_{\odot}$ of ^{56}Co and 5 times the “solar” value of $^{57}\text{Co}/^{56}\text{Co}$ (“solar” actually refers to the solar isotopic ratio of the radioactive cobalt daughter products $^{57}\text{Fe}/^{56}\text{Fe} = 0.024$). This conclusion was weakened by the fact that the critical data on day 1350 at 10 and $20 \mu\text{m}$, which are where the flux distribution peaks, were quite noisy, and in the case of the $20 \mu\text{m}$ data, we could only quote an upper limit. We have obtained further observations to tie down the late-time bolometric evolution of SN 1987A.

2. OBSERVATIONS

We have measured broad-band *UBVRI* magnitudes for days 1490 through 1600 from CCD data taken on the CTIO 0.9 m telescope, obtained at roughly monthly intervals, and measured with point-spread-function fitting techniques to exclude the light from the nearby stars in this crowded field.

¹ Cerro Tololo Inter-American Observatory, National Optical Astronomy Observatories, Casilla 603, La Serena, Chile, NOAO is operated by the Association of Universities for Research in Astronomy, Inc., under cooperative agreement with the National Science Foundation.

² Department of Astronomy, Ohio State University, Columbus, OH 43210,

The data through day 1470 and a discussion of the errors in the optical magnitudes is given in Walker & Suntzeff (1991). Near-infrared *JHK* magnitudes were measured on days 1444 and 1591 with the InSb infrared imager on the CTIO 4 m telescope. The *JHK* images were reduced as in S91, with the exception that for the later images, star 2 was employed as a local standard. The mean magnitudes for star 2 in this case were derived from S91 and the observations of day 1444, and the overall accuracy of the results in these cases is lower.

The mid-infrared 10 and $20 \mu\text{m}$ data were taken using the same setup as data previously reported for SN 1987A in S91. Data were taken with the CTIO 4 m telescope on each of three nights during a single run (day 1444), for total integration times at 10 and $20 \mu\text{m}$ of approximately 4 and 6 hr. In addition to the supernova measurements, faint A-type standard stars whose extrapolated 10 or $20 \mu\text{m}$ magnitudes were similar to those of SN 1987A were also observed, in order to confirm our ability to make accurate measurements at very low flux levels. The results of these latter measurements agreed, to within their uncertainties, with the predicted magnitudes.

The optical and mid-infrared evolution of SN 1987A is presented in Figure 1, where, for the mid-infrared, we have combined the CTIO data from S91, the ESO data (Bouchet et al. 1991a), and the new data corresponding to day 1444. The new optical and infrared magnitudes are given in Table 1, with the uncertainties quoted in units of hundredths of a magnitude.

3. DISCUSSION

Figure 1 shows the well-discussed behavior of SN 1987A through day 900. Over the first week, the *U* and *B* magnitudes dimmed rapidly as the supernova cooled. From about day 20 through day 120, a diffusion wave of energy was released by the rapid decay of $0.07 M_{\odot}$ of radioactive ^{56}Ni into ^{56}Co (e-folding decay time $t_e = 8.8$ days) behind the expanding supernova photosphere. From day 120 to day 500, the supernova was powered by the radioactive decay of ^{56}Co into ^{56}Fe , and all colors, except *U* and *B* which were affected by much higher opacities (Hamuy & Suntzeff 1990), fell at the rate close to that of ^{56}Co ($t_e = 111.3$ days). The bolometric luminosity fell at a rate of $t_e = 109.6 \pm 0.3$ days through day 300 (Bouchet et al. 1991b). From day 500 to 750, the optical and near-infrared fluxes suddenly fell while the 10 and $20 \mu\text{m}$ fluxes brightened as dust formed (Danziger et al. 1989), with the bolometric lumi-

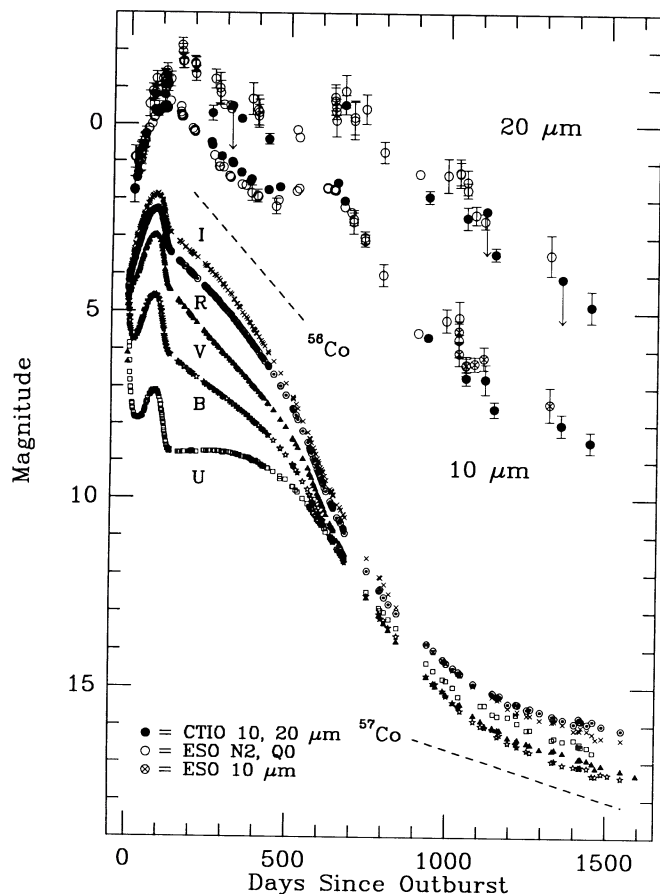


FIG. 1.—Broad-band photometric evolution of SN 1987A through day 1600 since outburst. The signature of three radioactive nuclides can be seen in the light curves: from day 40 to 100, the optical brightening was caused by the outward diffusion of the energy released by prompt decay of ^{56}Ni ; from day 120 to 500, the light curves fell at the ^{56}Co decay rate; and by day 1000, the light curves were falling at the ^{57}Co decay rate.

osity still tracking the ^{56}Co energy deposition into an increasingly transparent (to gamma rays) envelope (SB90). The bolometric evolution through day 900 has followed extremely well the early theoretical predictions (Woosley 1988; Woosley, Pinto, & Ensmann 1988; Kumagai et al. 1988), as well as the formation of dust around day 500 (Gehrz & Ney 1987).

The models (WPH89; Kumagai et al. 1989) for the late-time evolution of SN 1987A predict that after 1100, the energy deposition would be dominated by the radioactive decay of ^{57}Co into ^{57}Fe ($t_e = 391$ days), and, after day 1500, the radioactive decay of ^{44}Ti into ^{44}Sc ($t_e = 78$ yr) which decays immediately into ^{44}Ca . The only other radioactive nuclide predicted to form in abundance is ^{22}Na ($t_e = 3.8$ yr), and it is not expected to dominate the energy deposition at any time.

Figure 1 shows that all the optical light curves are falling at nearly the rate expected for ^{57}Co for days later than 1100. The average decline rate for $UBVI$ between days 1200 and 1600 (15 observations in each color) is 390 ± 20 days (m.e.), and for JHK between days 1100 and 1600 (four observations), 385 ± 20 days. The decline rate for the $10 \mu\text{m}$ data between days 1150 and 1450 (three observations) is 375 ± 80 days. The decline rate for the $20 \mu\text{m}$ data during the same period is somewhat less than 300 days, but the data are too sparse to allow a good fit. The R passband is falling somewhat more slowly at 540 days, and was not included in the averages since it is dominated by the single emission line of $\text{H}\alpha$. The similarity of all the decline rates over the period from day 1100 to 1600 provides strong evidence that the dominant energy source during this period must be ^{57}Co .

The broad-band data (U through $20 \mu\text{m}$) have been converted to equivalent monochromatic fluxes and integrated to estimate a bolometric luminosity. This technique and a discussion of the errors are given in SB90. The bolometric luminosities through day 1352 are given in S91. For day 1444, we find that $\log_{10}(L) = 37.05 \pm 0.2$ dex. Reasonable extrapolations into the ultraviolet including the ultraviolet flux reported from *HST* observations on day 1300 (Jakobsen et al. 1991) add less than $\sim 15\%$ to the flux on day 1350. The main uncertainty in the calculation of the bolometric luminosity is the extrapolation from $20 \mu\text{m}$ longward. We have done the extrapolation by fitting a scaled blackbody of 180 K to the mid-infrared data and added the flux longwards of $20 \mu\text{m}$ to the integration of the monochromatic fluxes. A blackbody as cool as $T_{\text{eff}} = 150$ K is also consistent with the data, a value preferred by the ESO group (Bouchet et al. 1991a) based on the ESO photometry including a detection of the supernova at 1.3 mm on day 1300. If the blackbody temperature is as low as 150 K, the bolometric flux will increase by 0.2 dex. If we assume the extrapolation is a Rayleigh-Jeans law scaled to the flux at $20 \mu\text{m}$, we find $\log(L) = 36.88 \pm 0.08$ dex. This latter estimate must be close to the lower limit, since the flux evolution of SN 1987A after day 500 clearly shows that dust formed and began to radiate as a cool blackbody (SB90).

The bolometric evolution of SN 1987A through day 1444 is plotted in Figure 2, along with the theoretical energy deposition from the four longer lived radioactive nuclides predicted to have formed in the supernova (WPH89; Kumagai et al. 1989). (Note that in Fig. 2 we have increased the predicted amount of ^{57}Co by a factor of 5 to fit the observed data.) The last bolometric data point, which includes measured fluxes from 3200 \AA to $20 \mu\text{m}$, is in excellent agreement with the data point on day 1350, and verifies that slowing of the decline rate is real. From Figure 2 it can be seen that even as early as day 750, another energy source besides ^{56}Co appears in the observed bolometric luminosity. The energy deposition from enhanced ^{57}Co clearly can account for this energy deficit.

TABLE 1
BROAD-BAND MAGNITUDES OF SN 1987A

Day	B	V	R	I	Day	J	H	K	10	20
1487.....	17.27	17.07	15.99	16.31	1444.....	15.32 (08)	15.28 (08)	15.25 (08)	8.5 (30)	4.8 (47)
1507.....	17.31	1591.....	15.75 (15)	15.66 (15)	16.10 (15)		
1547.....	17.39	17.21	16.11	16.37						
1594.....	...	17.34						

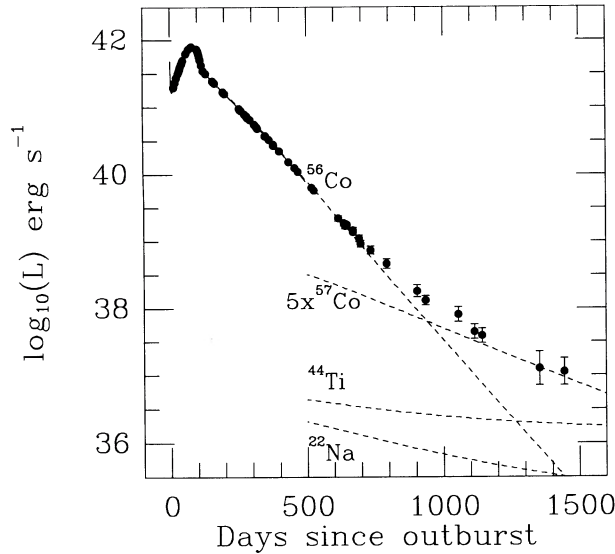


FIG. 2.—Bolometric evolution of SN 1987A through day 1444. The solid line from day 1 to 500 represents the estimates of the bolometric flux based on the U to M integration (see Suntzeff & Bouchet 1990), and the filled circles represents the U to $20\ \mu\text{m}$ integration. The dotted lines represent the estimates for the energy deposition (WPH89) for the four radioactive nuclides, except that the ^{57}Co has been raised to 5 times solar. The initial masses of these radioactive nuclides are: ^{56}Ni (and subsequently ^{56}Co), $0.075\ M_{\odot}$; ^{44}Ti , $1 \times 10^{-4}\ M_{\odot}$; ^{22}Na , $2 \times 10^{-6}\ M_{\odot}$; and ^{57}Co , $0.009\ M_{\odot}$ (5 times solar). By day 700, the observed bolometric flux is greater than the amount of energy deposited by ^{56}Co and another energy source is present.

From the early-time evolution of SN 1987A, we know the amount of ^{56}Ni (and its daughter ^{56}Co) synthesized in the explosion was $0.069 \pm 0.0012\ M_{\odot}$ (Bouchet et al. 1991b). In order to characterize the energy sources that dominate the late-time evolution, we have subtracted the energy deposition

that corresponds to $0.069\ M_{\odot}$ of ^{56}Co from the observed bolometric luminosity. In addition, in order to understand how the uncertainties in the assumed amount of ^{57}Co affect the results, we have also done the same calculation for the $3\ \sigma$ limits of ^{56}Co (0.073 and $0.065\ M_{\odot}$). All three calculations show that the non- ^{56}Co energy source declined by at least a factor of 20 from day 600 to 1500. The calculation for the $0.065\ M_{\odot}$ of ^{56}Co , however, gave a very large excess for days 600 to 800 that could not be fit by the models described below, so we have ignored this fit in the following discussion.

In Figure 3, we plot this energy “excess,” that is, the difference between the observed bolometric luminosity and the predicted energy deposition from 0.069 or $0.073\ M_{\odot}$ of ^{56}Co . One of the major conclusions to be drawn from Figure 3 is that the energy excess must be predominantly from an energy source that is exponentially declining in time. This is inconsistent with a constant energy source, such as that envisioned from a X-ray pulsar such as Her X-1 or SMC X-1, or an embedded radio pulsar similar to the Crab pulsar (WPH89; Kumagai et al. 1989). The energy deposition from an X-ray pulsar with the spectral energy distribution of Her X-1 or SMC X-1 is expected to decline by less than 40% from day 600 to 1500 due to the changing optical depth in the homologously expanding envelope. The Crab pulsar, which has a softer spectral energy distribution in the X-ray region, is expected to decline by a factor of 2.6 during this time interval as compared with an observed decrease of roughly a factor of 20.

The exponential decline shown in Figure 3 can be explained naturally by the energy deposition from a radioactive nuclide. The solid lines refer to the best fit to the data for the energy deposition from ^{57}Co (enhanced by factors of 5 and 6 over the predicted or “solar” value), and “solar” values for ^{44}Ti ($1 \times 10^{-4}\ M_{\odot}$) and ^{22}Na ($2 \times 10^{-6}\ M_{\odot}$). Over this time range, the latter two radioactive nuclides deposit negligible energy into the bolometric luminosity for such large enhance-

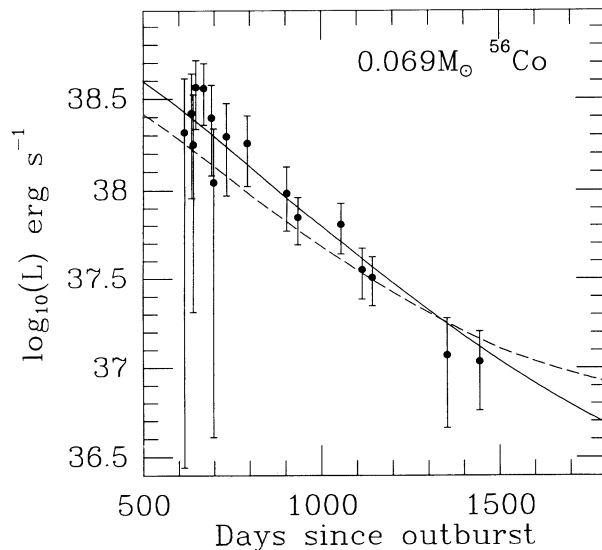


FIG. 3a

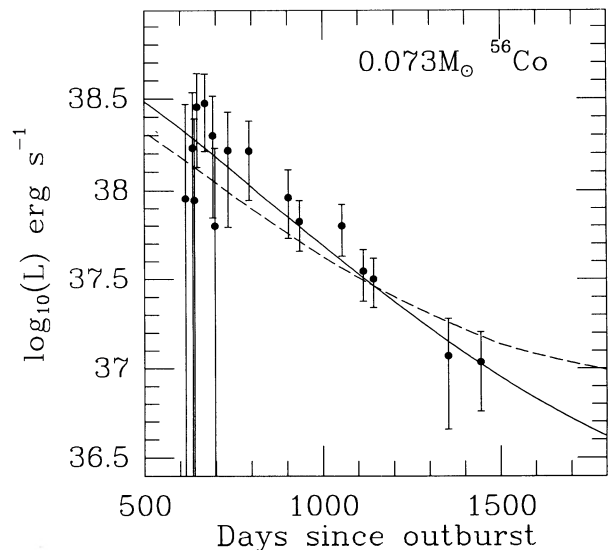


FIG. 3b

FIG. 3.—Difference between the observed bolometric flux and the predicted energy deposition from $0.069\ M_{\odot}$ (a) and $0.073\ M_{\odot}$ (b) of ^{56}Co . The solid lines are the energy deposition from enhanced ^{57}Co , and the dashed lines are the fits with the maximum pulsar luminosity (and thus minimum ^{57}Co energy deposition) consistent with the observed data. Note that the slope of the energy deficit is the same as the predicted energy input from ^{57}Co . The best-fit to the data without the pulsar is 6 times solar (a) and 5 times solar (b) of ^{57}Co . Using a pulsar with the energy spectrum of the Crab pulsar, the best fits are 4 times solar ^{57}Co plus a pulsar with a total spectral energy of 37.25 dex (a), and 3 times solar ^{57}Co plus 37.45 dex from a pulsar (b). The actual energy deposited by the pulsar is ~ 36.9 dex or less (see text).

ments of ^{57}Co . The second important conclusion from Figure 3 is that *the temporal behavior of this energy has the same slope to within the errors as the predicted deposition of ^{57}Co* . The similarity in *slope* is strong evidence that the energy excess is produced by ^{57}Co .

A fit to the data shown in Figure 3 yields an enhancement of ^{57}Co of 5 ± 1 . We estimate a lower limit to the enhancement of ^{57}Co of 3 times solar, in the case of a Rayleigh-Jeans extrapolation to the flux longwards of $20\ \mu\text{m}$. In Suntzeff et al. (1991), we reported that no more than 30% of the estimated bolometric luminosity could come from thermalized radiation from an echo. The images used in this present work were taken in poorer seeing, and we cannot improve on this estimate.

However, since the neutrino burst detected a few hours before the optical brightening is taken as compelling evidence that a neutron star formed (Arnett et al. 1989), we have also calculated the maximum possible energy deposition from a X-ray pulsar, by simultaneously increasing the pulsar energy and decreasing the energy input from ^{57}Co . We have used the predicted energy depositions for a Crab-like pulsar (WPH89), since it is predicted to have an energy deposition that is declining most rapidly in time for all the pulsar models. These fits, shown in Figure 3, are poorer fits to the data than the pure ^{57}Co model, and represent our best estimate for the maximum energy input from a pulsar, and conversely, the minimum amount of ^{57}Co . We find that the maximum possible energy input from a pulsar is ~ 37.45 dex for a minimum energy input from ^{57}Co at 3 times solar, in the case that $0.073\ M_{\odot}$ of ^{56}Co was formed. The value 37.45 dex represents the total luminosity of the X-ray pulsar spectrum, of which a fraction of 0.3 actually appears in the uvoir bolometric luminosity on day 1500. Had we chosen the X-ray deposition from Her X-1, the maximum total luminosity of the X-ray pulsar would be 37.1, of which 0.7 appears in the uvoir bolometric luminosity. For 100% energy deposition over the same time period, the upper limit would be 36.9 dex. Whereas the preceding tests show that the upper limit on the *deposited* energy from a pulsar is around $8 \times 10^{36}\ \text{ergs s}^{-1}$, the *total* energy radiated by the pulsar is poorly constrained since the nature of this radiation is unknown (see WPH89).

Since ^{44}Ti has such a long half-life, the energy deposition from the nuclide will mimic a constant energy source such as a pulsar. For the minimum amount of ^{57}Co at 3 times solar, 5 times solar ^{44}Ti would be needed to fit the data. This level of enhancement of ^{44}Ti however, is not supported by the models (Woosley & Hoffman 1991) which predict that ^{44}Ti is enhanced by 1.5 solar or less for enhancements of ^{57}Co of 3 times solar.

A factor of 5 enhancement of ^{57}Co is in disagreement with both the theoretical predictions (Woosley & Hoffman 1991; Kumagai et al. 1991), and published spectroscopic observations in the infrared (Danziger et al. 1991, Varani et al. 1990) and at X-ray energies (Sunyaev et al. 1991). The infrared observations, however, suffer from poorly determined ionization corrections and atomic constants, and we have argued elsewhere (S91) that the infrared spectral data cannot exclude ^{57}Co enhancements as large as 4 times solar. Similarly, the X-ray data are only upper limits, and errors in the estimates for the X-ray background could change the quoted levels of the upper limits. The theoretical limits on the production of ^{57}Co are based on the assumptions that ^{56}Ni be the dominant species of the iron group, that constraints on the neutron excess are given by the initial metallicity of the supernova progenitor, and that the ratio of $^{58}\text{Ni}/^{56}\text{Fe}$ not be more than a factor of 5 from the solar ratio (Woosley & Hoffman 1991). The production of copious amounts of ^{57}Co also requires the condition that the nucleosynthesis be dominated by the so-called "alpha-rich freeze out" from nuclear statistical equilibrium (nse); that is, the requirement that relatively low-density material in nse cools extremely rapidly so that the unbound α particles do not have time to capture back into the iron group elements. The theoretical limits on $^{57}\text{Co}/^{56}\text{Co}$ range from 0.5 to 2.5 solar. Relaxing the constraint on the $^{58}\text{Ni}/^{56}\text{Fe}$ ratio can bring the ^{57}Co up to a maximum of 4 times solar (Woosley & Hoffman 1991; Kumagai et al. 1991), but only by sacrificing the reasonable assumption that the isotopic ratios be close to the solar values. The *measured* abundance of nickel in SN 1987A (Danziger et al. 1991), corresponds to a ratio of $^{58}\text{Ni}/^{56}\text{Ni} = 0.7$ solar, if it is assumed that all the stable nickel is the most common isotope, ^{58}Ni . The measured nickel ratio in SN 1987A is therefore consistent with the assumption used in the models that this ratio be close to solar.

The resolution of the conflict between the theoretical requirement that the iron group elements have nearly solar abundance ratios and the compelling evidence that the radioactive decay of ^{57}Co now dominates the energy budget of SN 1987A (Figs. 1 and 3) will only be resolved by obtaining further data. As can be seen in Figure 3, by day 1800, the predicted energy depositions from enhanced ^{57}Co and the pulsar plus ^{57}Co are quite different. If ^{57}Co really is present at the levels implied here, we should expect the bolometric light curve to continue to fall until ^{44}Ti takes over as the dominant energy source, around day 2000. If however, there really is a pulsar (or enhanced ^{44}Ti) adding energy, the bolometric light curve can be expected to level off more quickly and at a higher energy.

REFERENCES

- Arnett, W. D., Bahcall, J. N., Kirshner, R. P., & Woosley, S. E. 1989, *ARA&A*, 27, 629
 Bouchet, P., Danziger, I. J., & Lucy, L. B. 1991a, *AJ*, 102, 1135
 Bouchet, P., Phillips, M. M., Suntzeff, N. B., Gouffes, C., Hanuschik, R. W., & Wooden, D. H. 1991b, *A&A*, 245, 490
 Danziger, I. J., Gouffes, C., Bouchet, P., & Lucy, L. B. 1989, *IAU Circ.*, No. 4746
 Danziger, I. J., Lucy, L. B., Bouchet, P., & Gouffes, C. 1991, in *Proc. of the Tenth Santa Cruz Summer Workshop, Supernovae*, ed. S. E. Woosley (New York: Springer), 69
 Gehrz, R. D., & Ney, E. P. 1987, *Proc. Natl. Acad. Sci.*, 84, 6961
 Hamuy, M., & Suntzeff, N. B. 1990, *AJ*, 99, 1146
 Jakobsen, P., et al. 1991, *ApJ*, 369, L63
 Kumagai, S., Itoh, M., Shigeyama, T., Nomoto, K., & Nishimura, J. 1988, *A&A*, 197, L7
 Kumagai, S., Shigeyama, T., Hashimoto, M., & Nomoto, K. 1991, *A&A*, in press
 Kumagai, S., Shigeyama, T., Nomoto, K., Itoh, M., Nishimura, J., & Tsuruta, S. 1989, *ApJ*, 345, 412
 Shigeyama, T., Nomoto, K., & Hashimoto, M. 1988, *A&A*, 196, 141
 Suntzeff, N. B., & Bouchet, P. 1990, *AJ*, 99, 650 (SB90)
 Suntzeff, N. B., Phillips, M. M., Depoy, D. L., Elias, J. H., & Walker, A. R. 1991, *AJ*, 102, 1118 (S91)
 Sunyaev, R. A., et al. 1991, in *Proc. of the Tenth Santa Cruz Summer Workshop, Supernovae*, ed. S. E. Woosley (New York: Springer), 767
 Varani, G.-F., Meikle, W. P. S., Spyromilio, J., & Allen, D. A. 1990, *MNRAS*, 245, 570
 Walker, A. R., & Suntzeff, N. B. 1989, *IAU Circ.*, No. 4881
 ———, 1991, *PASP*, 103, 958
 Woosley, S. E. 1988, *ApJ*, 330, 218
 Woosley, S. E., & Hoffman, R. 1991, *ApJ*, 368, L31
 Woosley, S. E., Pinto, P. A., & Ensmann, L. M. 1988, *ApJ*, 324, 466
 Woosley, S. E., Pinto, P. A., & Hartmann, D. 1989, *ApJ*, 346, 395 (WPH89)